Ahmad Bedram
Center of Excellence in Energy Conversion (CEEC),
School of Mechanical Engineering,
Sharif University of Technology,
Azadi Avenue, P.O. Box 11365-9567,
Tehran 11365-9567, Iran
e-mail: a_bedram@yahoo.com

Amir Ebrahim Darabi
Center of Excellence in Energy Conversion (CEEC),
School of Mechanical Engineering,
Sharif University of Technology,
Azadi Avenue, P.O. Box 11365-9567,
Tehran 11365-9567, Iran
e-mail: amir.adarabi@gmail.com

Ali Moosavi[1]
Associate Professor
Center of Excellence in Energy Conversion (CEEC),
School of Mechanical Engineering,
Sharif University of Technology,
Azadi Avenue, P.O. Box 11365-9567,
Tehran 11365-9567, Iran
e-mail: moosavi@sharif.edu

Siamak Kazemzade Hannani
Professor
Center of Excellence in Energy Conversion (CEEC),
School of Mechanical Engineering,
Sharif University of Technology,
Azadi Avenue, P.O. Box 11365-9567,
Tehran 11365-9567, Iran
e-mail: hannai@sharif.edu

Numerical Investigation of an Efficient Method (T-Junction With Valve) for Producing Unequal-Sized Droplets in Micro- and Nano-Fluidic Systems

We investigate an efficient method (T-junction with valve) to produce nonuniform droplets in micro- and nano-fluidic systems. The method relies on breakup of droplets in a T-junction with a valve in one of the minor branches. The system can be simply adjusted to generate droplets with an arbitrary volume ratio and does not suffer from the problems involved through applying the available methods for producing unequal droplets. A volume of fluid (VOF) based numerical scheme is used to study the method. Our results reveal that by decreasing the capillary number, smaller droplets can be produced in the branch with valve. Also, we find that the droplet breakup time is independent of the valve ratio and decreases with the increase of the capillary number. Also, the results indicate that the whole breakup length does not depend on the valve ratio. The whole breakup length decreases with the decrease of the capillary number at the microscales, but it is independent of the capillary number at the nanoscales. In the breakup process, if the tunnel forms the pressure drop does not depend on the valve ratio. Otherwise, the pressure drop reduces linearly by increasing the valve ratio. [DOI: 10.1115/1.4028499]

Keywords: unequal-sized droplets, T-junction with valve, numerical simulation, VOF, nano, 3D

Introduction

Droplet based micro- and nano-fluidic systems have found various applications in many industries. These systems allow one to prevent important fluids, such as the components of drugs, from pollution or chemical reaction with the other materials by encapsulating them in droplets that are buoyant in a base fluid [1]. Also, these systems have many other advantages such as better mixing of the reactants that are inside the droplets due to the circulation of the flow inside the droplets [2]. In these systems, processes, such as the formation [3–6], deformation [7], breakup in symmetric [8] and asymmetric [9,10] geometries, coalescence [11], mixing, and transport [12] of droplets, occur. Therefore, many investigations have been conducted to study these processes over the last decade [10–17].

For production of emulsions that have many applications in chemical and pharmaceutical industries, it is required to rapidly generate a large number of droplets in various sizes. Therefore, effective methods should be available for this purpose. Various methods have been proposed for high speed generation of equal-size droplets [8,10,18]. These methods have a basic disadvantage as they generate only one size of droplets. The industries, such as pharmaceutical industry, produce materials with widespread range of components and sizes. These components may be in the form of large droplets initially. Then, these droplets are divided into very smaller parts that each one is used in a product, for example, in a tablet. In these situations, if we apply the methods that generate equal-size droplets, it will be necessary to employ a suitable system for producing smaller droplets from those droplets. In the last decade, several methods have been proposed that produce unequal-sized droplets from an initial one. The main advantage of these methods is that the droplets with various sizes can be generated using these systems alone. However, as will be explained in the next paragraphs, the available methods have some disadvantages. Clearly, reducing the disadvantages of the available methods and resolving their problems is an important task.

There are only few methods suggested for generating unequal-sized droplets. Link et al. [10] have proposed two methods for generating unequal-sized droplets. One of their methods relies on using an obstacle inside a straight channel. The main disadvantage of this method is that after generating large and small droplets, the produced small and large droplets move together along the channel and for separation of them a different process is required. The other method of Link et al. [10] is a T-junction with unequal length branches. In this method, the volume ratio of the generated droplets has an inverse relation with the length ratio of the branches ($V_1/V_2 \approx l_2/l_1$, where V is the volume of droplet, l is the length of the branch, and the subscripts 1 and 2 represent each of the two branches). In this method, for the cases with high volume ratios, the length of the branches should be increased and this increases both the manufacturing cost and the pressure drop in the system. Sehgal et al. [19] investigated a droplet that goes up inside a vertical tube and breaks up into unequal smaller droplets at a Weber number larger than 5. The disadvantage of this method is that the produced small and large droplets move together along

[1]Corresponding author.

Contributed by the Fluids Engineering Division of ASME for publication in the JOURNAL OF FLUIDS ENGINEERING. Manuscript received March 16, 2014; final manuscript received September 2, 2014; published online October 21, 2014. Assoc. Editor: Daniel Maynes.

the channel. Deremble and Tabeling [9] used a T-junction with branches with arbitrary angle (Y-junction). This method has the disadvantage of Link et al. method [10]. Choi et al. [20] have introduced a new method for generating unequal-sized droplets. They have used a pneumatic valve in a tube consisting of a continuous fluid and consecutive droplets. The pneumatic valve has a constant pressure and when a droplet passes through it breaks up into two unequal-sized droplets based on the magnitude of the pressure of the pneumatic valve. Their method has two disadvantages. The main disadvantage is that the generated small and large droplets move along in the channel. Therefore, an additional process is required for separating them. Another disadvantage of their method is that for generating droplets with a specified volume ratio, the pressure of the valve should be kept constant because a small change in the pressure changes the volume ratio. Providing this condition is difficult as the presence of the droplet in the valve location changes the pressure.

Ting et al. [21] have proposed a heat transfer based method. A heater is considered in one of the branches of a symmetric T-junction. In the branch with heater, the temperature of the fluid increases and the hydrodynamic resistance reduces. Therefore, the size of the droplet that enters this branch becomes smaller than the droplet of the other branch. However, the applicability of this method is limited. If in the heated branch there is a low pressure region in this region, the temperature of the liquid that is increased by heater may exceed the limiting value. This problem occurs in large capillary numbers and low volume ratios. In these conditions, heat transfer should be increased. For production of a specific volume ratio by increasing the capillary number, the difference between the hydrodynamic resistances of the two branches increases [21]. Thus, for this condition, the temperature reaches to values larger than 40 °C reported in Ref. [21] and this limits its applications, for instance, for biological applications. A T-junction with unequal width branches has been also studied by Bedram and Moosavi [22]. Their system requires a small length for the branches for all the new volume ratios and does not have the disadvantage of the method proposed by Link et al. [10].

Dupin et al. [3] proposed a method that generates droplets with a specific size but their method does not work based on the breakup of droplets. In the breakup problems, there is an initial droplet that is carried by a fluid and this droplet is divided into two or more parts with equal or unequal sizes because of passing through, for example, a T-junction with valve. Also, the method of Dupin et al. can generate only one size of droplets (see Fig. 4 of Dupin et al.) but a T-junction with valve can divide the initial droplet into two unequal-sized parts.

Liu and Zhang [4,5] and Wu et al. [6] investigated droplet formation using cross junctions. The cross junction method can only generate droplets from the initial fluids and does not able to breakup an initial droplet to smaller parts.

There are some other methods such as breakup of bubble in turbulent flow using a simple shear flow and T-junctions with branches with different length [23]. All of the mentioned methods have one or more problems similar to those of the methods of Link et al.

In the present study, we attempt to study in detail a system that does not have some of the problems reported for the available methods [24]. In this system, a T-junction with a valve in one of its branches has been used for producing unequal-sized droplets. In this system, not only the produced droplets have been separated from each other after the breakup but also after manufacturing the system the size of the droplets can be simply changed. Moreover, the problem of vaporization of the fluid, which occurs in the heat transfer based methods, does not exist. The employed method for the study is the numerical simulation based on a VOF scheme. We investigate the influence of the capillary number and geometrical parameters (i.e., the valve ratio) on important performance parameters of the system such as the breakup time, the breakup length, and the pressure drop.

The System Characteristics

A schematic representation of the system for producing unequal-sized droplets is depicted in Fig. 1. As illustrated, the system consists of a T-junction with a valve in one of the branches. The valve is in fact represented by an orifice plate with width h as indicated in the right branch of Fig. 1. It is assumed that the valve is completely rigid and also does not vibrate due to the fluid flow. In this method, an initial droplet is introduced into the system by a carrier fluid from an inlet channel. When the droplet reaches to the junction, it either deforms asymmetrically and breaks into two parts with each entering one of the branches or does not break and enters the branch that does not have valve.

In Fig. 1, U and u stand for the mean velocity of the carrier fluid in the inlet channel and branches, respectively. In Fig. 1, U_{in}, u_1, and u_2 represent the mean velocity of carrier fluid in the inlet (vertical) tube, the branch with valve, and the branch without valve, respectively. The widths of all the channels are the same and equal to w. The simulations have been performed for both 2D and 3D dimensions and the results are compared. The geometry for 3D system is similar to that illustrated in Fig. 1 and the cross section of all the channels is a $w \times w$ square. Figure 2 depicts the geometry of the considered system in 3D mode. In 2D and 3D dimensions, we have $0 < h < w$.

Numerical Algorithm

The problem is simulated using an in-house code based on the numerical methods of Ref. [25]. The method that uses the VOF algorithm can be briefly described as follows.

Two nonvolatile, incompressible, and immiscible fluids were considered and the required equations with the associated boundary conditions were solved for the system. The continuity equation for the system is given by

$$\frac{\partial u_i}{\partial x_i} = 0 \tag{1}$$

with u_i as the velocity vector. The momentum equation for the system can be represented by

$$\rho\left(\frac{\partial u_i}{\partial t} + u_j \frac{\partial u_i}{\partial x_j}\right) = \frac{\partial P}{\partial x_i} + F_i + \mu \frac{\partial^2 x_i}{\partial x_j^2} \tag{2}$$

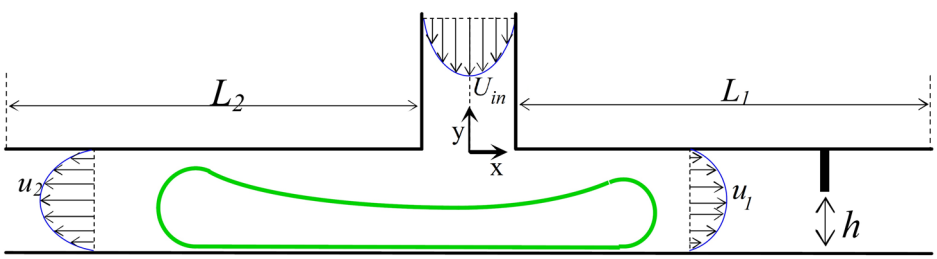

Fig. 1 The geometry of the T-junction with valve and representation of the involved parameters

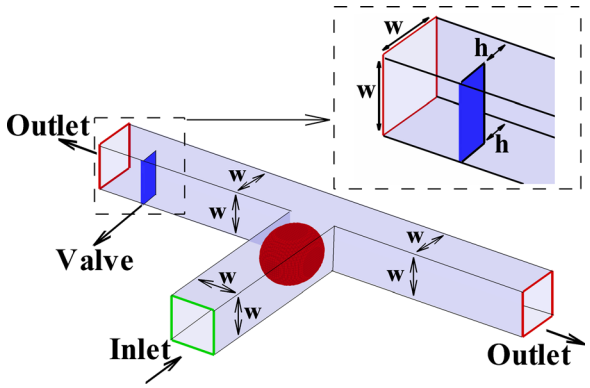

Fig. 2 3D configuration of the system

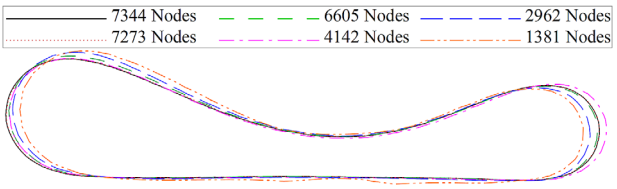

Fig. 3 Checking the grid independency of the results. The droplet deforms and breaks up into two parts. In this case, Ca = 0.04 and volume ratio = 0.6 and the droplet is in the center of the junction. The grids that have more than 6605 nodes are confident and we use the grid with 11,542 nodes for simulation of our cases.

where ρ and μ are the average density and viscosity, respectively, and their values can be calculated from the volume fraction of the continuous phase ϕ and the density and viscosity of the continuous (specified by subscript c) and the dispersed (specified by subscript d) phases from the following equation:

$$\rho = \rho_c\phi + \rho_d(1-\phi) \tag{3}$$

$$\mu = \mu_c\phi + \mu_d(1-\phi) \tag{4}$$

In all the computational cells, we have $0 \le \phi \le 1$. When $\emptyset$ is equal to one, the cell is occupied completely by the continuous and $\emptyset = 0$ means that the cell is fully filled with the dispersed phase. If the volume fraction is not equal to its maximum (1) or minimum (0) value, it means that the cell is occupied by both the phases and the boundary of the dispersed phase passes through that cell. $\emptyset$ is derived from the following equation:

$$\frac{\partial\phi}{\partial t} + \mathrm{u}_i \cdot \frac{\partial\phi}{\partial x_i} = 0 \tag{5}$$

The location of the interface is considered to be positions with $\phi = 0.5$ that is calculated with a piecewise linear interface reconstruction method. In Eq. (2), the effect of the surface tension force F_s is given by

$$F_i = \gamma\kappa\delta_s\hat{n}_i \tag{6}$$

where γ stands for the interfacial tension and κ represents the mean curvature of the interface. Also, δ_s and $\hat{n}_i$ stand for the delta function and the interface unit normal vector, respectively. For the cells near the wall, the normal vector can be calculated using the following relation:

$$\hat{n}_i = \hat{\mathrm{n}}_w \cos\theta + \hat{\mathrm{t}}_w \sin\theta \tag{7}$$

where $\hat{\mathrm{n}}_w$ and $\hat{\mathrm{t}}_w$ are the unit vectors normal and tangential to the wall surface, respectively, and θ is the contact angle.

The time step and the grid size are selected such that the results do not depend on the number of nodes and the time interval. We considered 9007 and 530,280 nodes for 2D and 3D dimensions, respectively. The time step size was also considered to be 2×10^{-7}s. For checking the grid and time step independencies, we considered the droplet shape in a state similar to Fig. 6(*b*). The droplet deforms in the center of the junction. In this state, we compared the shape of the droplet for various grid sizes. The results are shown in Fig. 3. As seen, for grids with more than 6605 nodes, the changes in the results are very small. Discretization of the momentum equations is done with the Quadratic Upstream Interpolation for Convective Kinematics (QUICK) method. Also, for pressure velocity decoupling, the Semi-Implicit Method for Pressure-Linked Equations (Consistent) (SIMPLEC) algorithm is used. The convergence criterion is considered to be reached, when the residuals are smaller than 0.0005. The residuals are defined by the following equation:

$$R_\phi = \frac{\sum_{P=1}^{N}\left|\sum_{nb} a_{nb}\phi_{nb} + \chi - a_P\phi_P\right|}{\sum_{P=1}^{N} a_P\phi_P} \tag{8}$$

where ϕ is a general variable at a cell P, N denotes the number of cells in the computational domain, nb represents the neighboring cells of the cell P, and χ is the constant part of the source term ($S = S_c + S_P\phi$) and of the boundary conditions.

In the study, capillary number is defined as $\mathrm{Ca} = \mu_e U_{in}/\gamma$, where μ_e is the viscosity of the carrier fluid, γ represents the surface tension between two fluids, and U_{in} denotes the mean velocity of the carrier fluid in the entrance of the system. Physically, the capillary number represents the ratio of the inertial to the capillary forces.

For verification of accuracy of our numerical scheme, a symmetric T-junction simulated. In these simulations, the boundary conditions for the inlet, the walls, and the outlets were the constant velocity, the no-slip, and the constant pressure, respectively. 5750 nodes were considered for modeling the system. Droplet sizes were from $1.2w$ to $6.6w$ with w as the channel width. The density and the viscosity of the main fluid that carries the droplets are 800 kg/m^3 and 0.00125 Pa·s, respectively, and the density and viscosity of the droplets are 1000 kg/m^3 and 0.001 Pa·s, respectively. The surface tension between the two fluids was assumed to be 0.005 N/m. Leshansky and Pismen [8] have derived an analytical relation between critical length of droplet[2] and capillary number in a symmetric T-junction as $l/w = 1.3\mathrm{Ca}^{-0.21}$. The numerical results of the mentioned T-junction have been compared with the analytical results in Fig. 4.

Bretherton [26] developed the following relation by means of an analytical theory for the velocity of a droplet that moves through a simple circular tube due to the flow of the carrier fluid:

$$U = \bar{U}\left(1 + 1.29\left(\frac{\mu_c U}{\gamma}\right)^{2/3}\right) \tag{9}$$

where U is the droplet velocity; $\bar{U}$ and μ_c represent mean velocity and viscosity of the continuous fluid, respectively; and γ is the surface tension coefficient. The same problem was considered for verifying the numerical algorithm, namely, a simple circular tube with a droplet inside it. The length of the droplet was supposed to be twice the channel diameter. The constant velocity, the no-slip, and the constant pressure were used as the boundary conditions for the inlet, the walls, and the outlets, respectively. In total, 2450 nodes were considered. The density and the viscosity of the continuous fluid (that carries the droplets) are 800 kg/m^3 and

[2]For the initial lengths of the droplet that are smaller than a specific value (critical length), the droplet doesn't break.

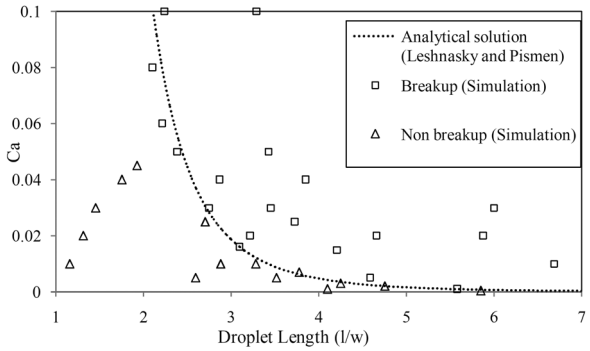

Fig. 4 Droplet critical length as a function of capillary number. Dotted line is the analytical relation ($l/w = 1.3\mathrm{Ca}^{-0.21}$). The critical length became dimensionless by width of channel.

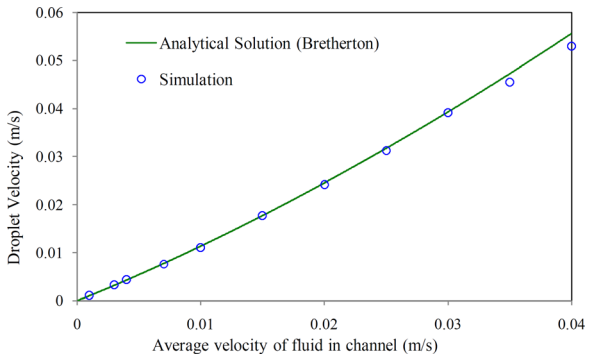

Fig. 5 Droplet velocity as a function of mean velocity of carrier fluid in tube. In the values of mean velocity of carrier fluid larger than 0.03, a small difference exists between the analytical and numerical results. It is because that the analytical results are derived by assumption of low value of carrier fluid mean velocity.

0.002 Pa·s, respectively, and density and viscosity of the droplets are 1000 kg/m^3 and 0.001 Pa·s, respectively. The surface tension between two the fluids is equal to 0.005 N/m. Figure 5 illustrates the comparison of the analytical relation of Bretherton and the numerical results. In both Figs. 4 and 5, a very good agreement exists between the numerical and the analytical results.

Results and Discussion

In this section, the results for production of unequal-sized droplets from an initial droplet in the T-junction with a valve are given. The results have been presented for micro- and nanoscales cases in different parts. In order to provide a comparison, the simulations have been conducted for both 2D and 3D systems.

Micro T-Junction With Valve. A sample of breakup process in the system is depicted in Fig. 6. The constant velocity, the no-slip, and the constant pressure were considered as the boundary conditions for the inlet, walls, and outlets, respectively.

In the simulations, it is assumed that the lengths of the branches are equal. Also the widths of the branches are supposed to be equal to that of the inlet channel. The valve ratio is defined as the opening percent of the channel, i.e.,

$$\text{valve ratio} = \frac{h}{w} \tag{10}$$

where h is the valve height as explained in Fig. 1. If the valve ratio is equal to 1, the valve is completely open and we have a symmetric T-junction. The droplet volume ratio is defined as the ratio of

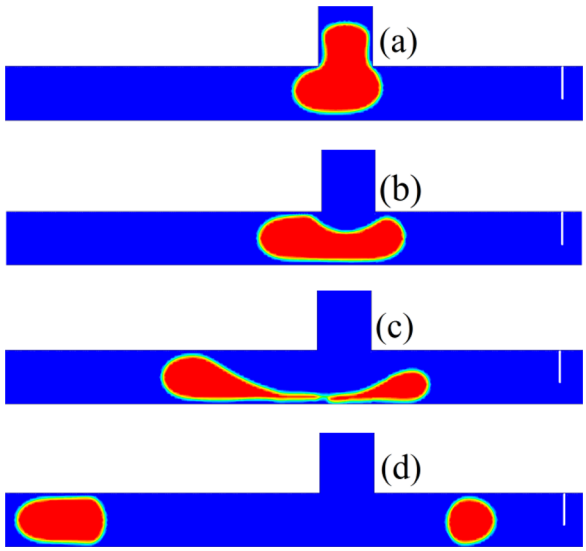

Fig. 6 The breakup process of unequal-sized droplets. For the shown case, the capillary number is 0.1, the valve ratio is 0.4, and the volume ratio is 0.48.

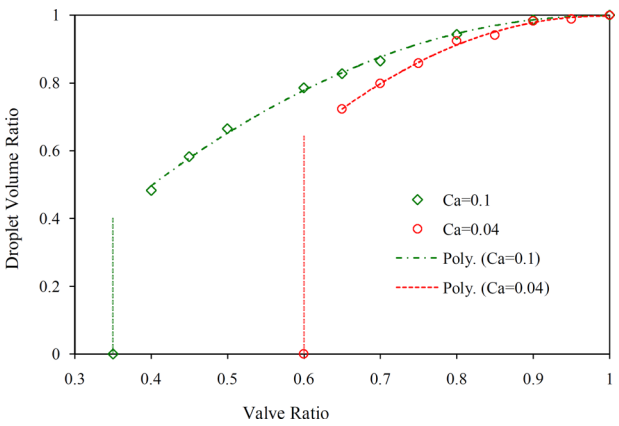

Fig. 7 Droplet volume ratio as a function of the valve ratio and the capillary number. When the valve ratio is equal to 1 (symmetric T-junction), the droplets that enter the branches have the same size. Also for a specific volume ratio as the capillary number decreases, the valve should be opened further and, as a result, the T-junction becomes more symmetric.

the volume of the smaller droplet (that enters the minor branch with valve) to the volume of the larger droplet (that enters the other minor branch).

Figure 7 shows the droplet volume ratio as a function of the valve ratio for two capillary numbers. An examination of the figure reveals the following three points: First, by increasing the valve ratio and the capillary number, the droplet volume ratio increases. Second, for each capillary number, the vertical line shows the valve ratio below that no droplet enters the minor branch with the valve. Finally, in a specific valve ratio, by decreasing the capillary number, smaller volume ratios can be achieved.

In many applications of symmetric and asymmetric T-junctions, droplets are transported through consecutive T-junctions. Figure 8 illustrates an example of such a process. In the first T-junction of Fig. 8 with the decrease of the distance between two consecutive droplets (before the junction), more droplets can pass through the T-junction in a specific time; therefore, the rate of the droplet generation increases. Let X be the distance between two consecutive droplets before the first T-junction

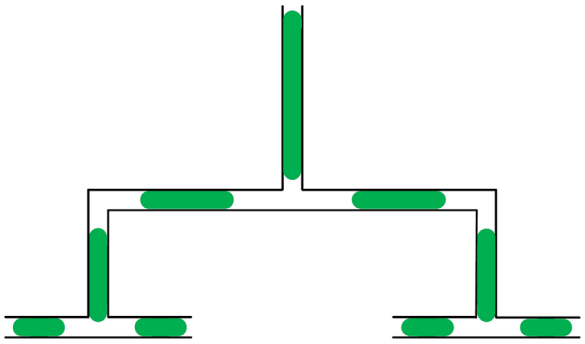

Fig. 8 Generation of equal-size droplets using consecutive symmetric T-junctions

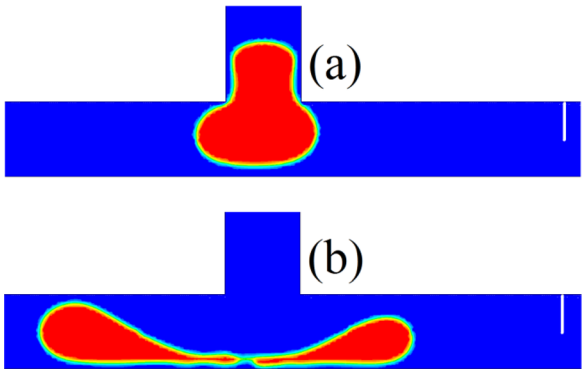

Fig. 9 $t_{breakup}$ is the time between the situation displayed in part (*a*) and part (*b*). The valve ratio is equal to 0.5 and the capillary number is Ca = 0.1.

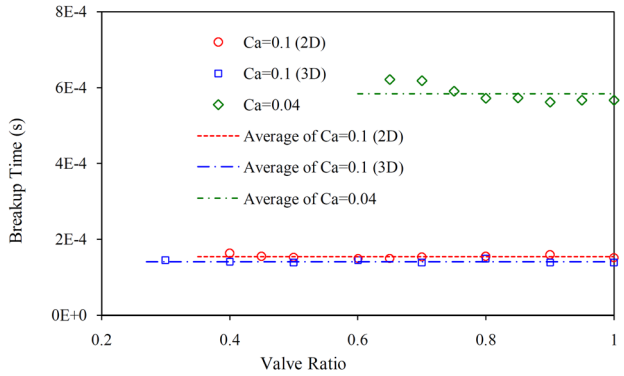

Fig. 10 Breakup time as a function of valve ratio. The average value of breakup time for Ca = 0.04, Ca = 0.1 (2D), and Ca = 0.1 (3D) are 5.84×10^{-4}, 1.55×10^{-4}, and 1.41×10^{-4} (second dimension), respectively.

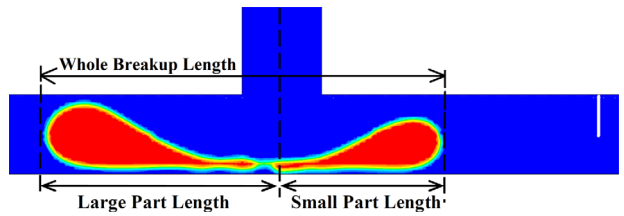

Fig. 11 Droplet breakup length. The vertical dashed line (in the junction center) is the centerline of the inlet channel. The whole breakup length, namely, the length of the droplet at the breakup moment, is composed of the large part length and the small part length.

in Fig. 8. Also, U is the velocity of the droplets that are before the first T-junction. As long as the first droplet has not completed the breakup process, the second one should not reach the T-junctions; in this condition, the second droplet will affect the breakup process of the first droplet. Thus, we have

$$X_{\min} = U_{\text{droplet}} \times t_{\text{breakup}} \tag{11}$$

where t_{breakup} is droplet breakup time, namely, the time between the moment that droplet arrives at the junction (Fig. 9(*a*)) and the moment that the droplet breaks up (Fig. 9(*b*)). Usually, we cannot control U, and it depends on the process and application; therefore, we can minimize X (and maximize droplet production rate) with minimization of t_{breakup}. Hence, we should study the variations of t_{breakup} in different conditions to find its minimum.

Figure 10 illustrates the breakup time as a function of valve ratio in two different capillary numbers. As seen, the breakup time in each capillary numbers is independent of the valve ratio and has a constant value, but decreases with the increase of the capillary number. Therefore, for reduction of breakup time (decrease of $X_{\min}$) and increase of droplet generation rate, the capillary number should be increased as much as possible. Also, in Fig. 10(*a*), comparison is done in Ca = 0.1 between 2D and 3D simulation results. As seen, the 2D and 3D results are very close. The average of breakup time in 2D and 3D cases is 1.55×10^4 and 1.41×10^4, respectively. Therefore, 2D and 3D cases have approximately 9% difference.

In Fig. 8, after each T-junction, there is a 90 deg elbow. As the distance between the elbow and the junction reduces, a shorter tube is consumed; the cost of system manufacturing decreases. The minimum distance between the junction and the elbow can be equal to a value that the droplet does not reach to the elbow until the end of breakup process. Otherwise, the elbow can change the breakup process. Therefore, for finding the minimum distance between the elbow and the junction, it is necessary to find the distance between the ends of the droplet and the junction center at the breakup moment in different conditions that we name this distance "droplet breakup length" and is explained in Fig. 11. Because of breaking the initial droplet into two unequal parts, there exist two breakup lengths, namely, breakup length of the large part and breakup length of the small part that is explained in Fig. 11.

Figure 12 displays the breakup length as a function of valve ratio in two capillary numbers. Also, in Ca = 0.1, results of both 2D and 3D cases are seen. An examination of the figure reveals that with the reduction of the valve ratio the breakup length of smaller (larger) droplet decreases (increases). This happens because a smaller (larger) quantity of droplet enters the branch with (without) valve. Since both the branches have the same length and width, we should minimize the summation of breakup length of the branches, namely, whole breakup length (Fig. 11). The summation of breakup length of the branches is shown in Fig. 12 and its name is "whole length of droplet." As can be seen in Fig. 12, the whole length of the droplet is independent of the valve ratio but decreases with reduction of the capillary number. The average of the whole length of the droplet in the cases Ca = 0.04, Ca = 0.1 (2D), and Ca = 0.1 (3D) are 4.49, 5.03, and 5.36, respectively. Also, Fig. 12 shows that the breakup lengths for 2D and 3D cases are very close (6.6% difference in whole length of the droplet).

In the fluidic systems, the pressure drop is one of the most effective parameters on the cost of system. Therefore, in the mentioned system, the pressure drop was investigated. The pressure drop was calculated at the moment that the droplet breaks up (Fig. 9(*b*)). In this situation, we define the "pressure drop" as the difference between the pressure of the carrier fluid in the inlet and the outlet of the system.

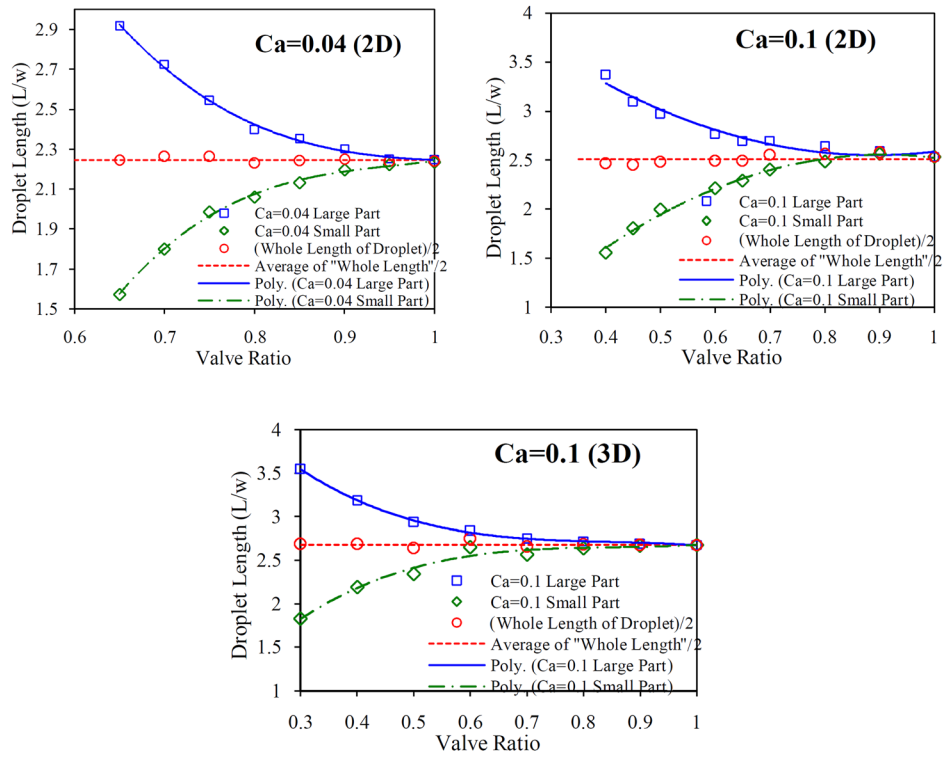

Fig. 12 Breakup length as a function of valve ratio. The breakup length of droplet is dimensionless (*w* is the width of the branches). For the valve ratio near 1 (symmetric T-junction), in each capillary number, the droplets that enter the branches have the same size; therefore, the breakup lengths of them are equal.

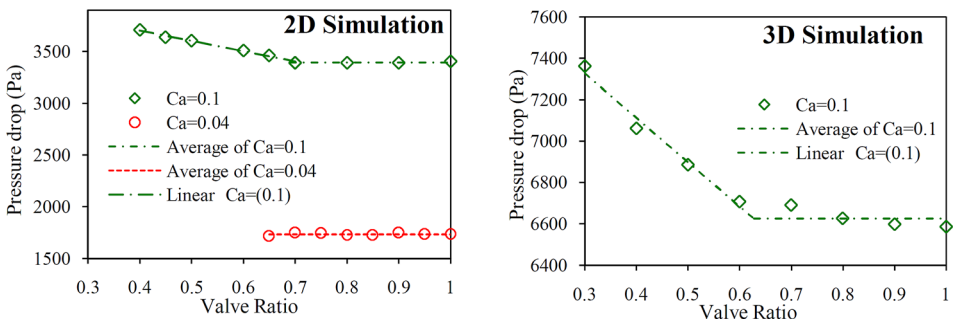

Fig. 13 Pressure drop as a function of valve ratio. In the above diagram, the pressure drop is calculated at the breakup moment. The results have shown that approximately at this moment the maximum pressure drop occurs.

Figure 13 depicts the pressure drop as a function of valve ratio in two different capillary numbers. As seen in Fig. 13, the pressure drop is independent of the valve ratio (except valve ratio < 0.7 in $Ca = 0.1$). In the case of $Ca = 0.1$ (in both 2D and 3D cases) and valve ratio < 0.7, the pressure drop reduces linearly with the increase of valve ratio. This is because, in $Ca = 0.1$ and valve ratio > 0.7, in the breakup moment, a distance forms between the upper interface of larger droplet (the droplet that enters the branch without valve) and the upper wall. We named this distance "tunnel" that carrier fluid pass through it (Fig. 14).

In $Ca = 0.1$ and the valve ratio < 0.7, the tunnel width starts to thinning. With thinning of the tunnel, the pressure drop increases linearly with reduction of the valve ratio. Therefore, in the considered system, in situations that the tunnel forms, the pressure drop is independent of the valve ratio and in the states that tunnel does not forms, the pressure drop increase linearly with the reduction

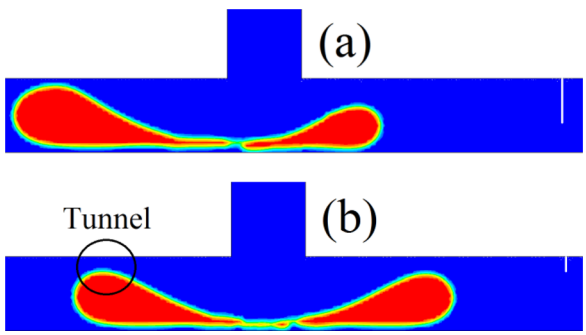

Fig. 14 Droplet breakup. (*a*) without tunnel, Ca = 0.1 and valve ratio = 0.4. (*b*) with tunnel, Ca = 0.1 and valve ratio = 0.8.

of the valve ratio. In Ca = 0.04, the tunnel forms in all the valve ratios. Therefore, for Ca = 0.04 in Fig. 13, the pressure drop is constant. Also, with the increase of capillary number, the pressure drop increases. Therefore, it can be concluded that for a specific capillary number for reduction of pressure drop (particularly for large capillary numbers) the valve ratio should be chosen large enough such that the tunnel is formed.

Also, Fig. 13 indicates that 2D and 3D results are very close. In both 2D and 3D results for Ca = 0.1, in the valve ratios near the 0.7, the sudden change in the pressure drop curve occurs. The difference between the values of the pressure drop in 2D and 3D systems is because of the hydraulic diameter difference ($2w$ in the 2D case and w in the 3D case, where w is the channel width).

Nano T-Junction With Valve. In this section, we reduce the channel size to nanometer scales. However, we keep the size large enough such that the continuity assumption is still valid. The Navier–Stokes equations are valid for fluid flow in continuum condition. For checking the continuum assumption, we calculate the Knudsen number (Kn), which is defined as

$$\mathrm{Kn} = \frac{\lambda}{l} \tag{12}$$

where λ is mean free path of the fluid molecules and l is the characteristic length. For liquids, λ approximately is equal to intermolecular length (L_{mol}) [27], and we have

$$L_{\mathrm{mol}} = \left(\frac{M}{\rho N_{\mathrm{A}}}\right)^{1/3} \tag{13}$$

where M, N_{A}, and ρ are molecular mass, Avogadro number, and density of liquid, respectively. The influence of Kn on the governing equations and boundary conditions is given as

(1) If Kn < 0.01, Navier–Stokes equations are valid (normal state).
(2) If 0.01 < Kn < 0.1, Navier–Stokes equations are valid but no-slip condition is not valid and we have slip condition in walls.
(3) If Kn > 0.1, the Navier–Stokes equations are not valid and the calculations should be conducted via a suitable method such as molecular dynamics.

For the considered fluids (oil and water), we have $L_{\mathrm{mol}} \approx 5 \times 10^{-9}$ m. The specific length in microcases is about 20×10^{-6} m and, as a result, one obtains Kn $\approx 2.5 \times 10^{-4}$. Therefore, the Navier–Stokes equations are applicable (with no-slip condition). Also, the specific length in nanocases is about 100×10^{-9} m (that is equal to width of the inlet channel) and, as a result, one obtains Kn ≈ 0.05. Therefore, the Navier–Stokes equations are applicable (with slip condition). For the slip boundary condition, Navier introduced the following relation [28]:

$$v_{\mathrm{s}} = \beta\left(\frac{\partial v}{\partial n}\right) \tag{14}$$

where β is the slip length, v_{s} represents the fluid velocity along the wall, and $\partial v/\partial n$ is the wall shear stress. For nanoscale cases, we consider a particular case in which the slip length is infinity ($\beta = \infty$). Therefore, from Eq. (14), we have $(\partial v/\partial n)_{\mathrm{wall}} = 0$. Thus, the wall shear stress was fixed to be zero.

In Fig. 15, the volume ratio is depicted as a function of valve ratio in the two capillary numbers. The channel width is equal to 100 nm. As seen, in a specific valve ratio, with the increase of the capillary number the droplet volume ratio increases. Also, if the valve ratio reduces from a specific value, the volume ratio reaches to zero, namely, no droplet enters the branch with valve. The

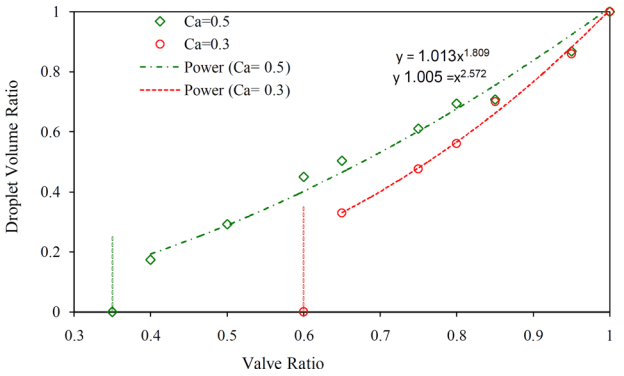

Fig. 15 Droplet volume ratio as a function of the valve ratio for two capillary numbers for the nanoscale case. In the valve ratio equal to 1, the equal-size droplets enter each branch and the volume ratio becomes 1. Also to obtain a specific volume ratio, if we select a smaller capillary number, the required valve ratio increases. This means that the junction becomes more symmetric.

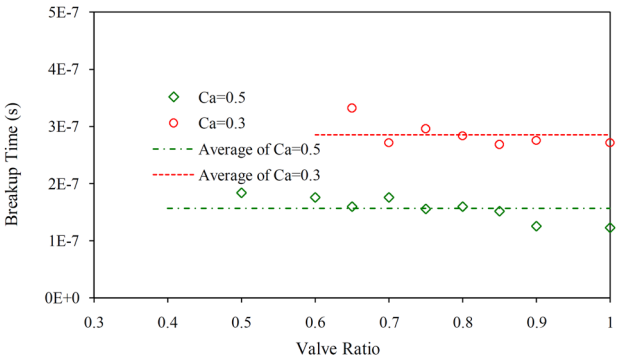

Fig. 16 Breakup time as a function of valve ratio for the nanoscale case. The average of the breakup time is 2.86×10^{-7} s and 1.57×10^{-7} s for Ca = 0.3 and Ca = 0.5, respectively.

mentioned specific value of valve ratio is 0.6 and 0.35 for Ca = 0.3 and Ca = 0.5, respectively.

Figure 16 indicates the breakup time as a function of valve ratio for capillary numbers 0.3 and 0.5. As seen, at the nanoscales, the breakup time is independent of the valve ratio and reduces with the increase of the capillary number. Therefore, for reducing the breakup time (decreasing of X_{min}) and increasing the droplet generation rate, the capillary number should be increased as much as possible.

Figure 17 illustrates the breakup length as a function of valve ratio in two capillary numbers. Already it was remarked that for minimization of system cost, the breakup length should be minimized. Figure 17 shows that the whole breakup length (whole length of droplet) is independent of the valve ratio. The interesting point is that the breakup length is approximately independent of the capillary number too. The average whole breakup length in Ca = 0.3 and Ca = 0.5 is 2.22 and 2.2, respectively (about 0.9% difference). Therefore, the breakup length at nanoscales does not alter appreciably by changing the capillary number and the valve ratio.

Figure 18 indicates the pressure drop as a function of valve ratio in different capillary numbers. As seen, with the increase of the valve ratio, the pressure drop reduces linearly. This is due to the tunnel formation problem, i.e., at the nanoscale case, in Ca = 0.3 and Ca = 0.5 in all of the valve ratios, the tunnel does not form (Fig. 19). Therefore, the pressure drop reduces linearly by increasing the valve ratio. Also, with the increase of capillary number, the pressure drop increases. Therefore, at the nanoscales,

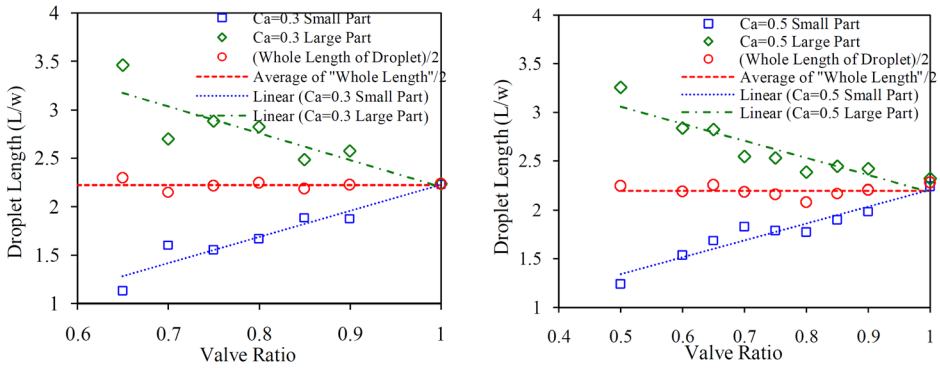

Fig. 17 Droplet breakup length as a function of the valve ratio for the nanoscale case. The breakup length is scaled by the channel width *w*. As it can be deduced, for the valve ratios near 1 (symmetric T-junction), for all the capillary numbers, the droplets that enter the branches have the same size. Therefore, their breakup lengths are equal.

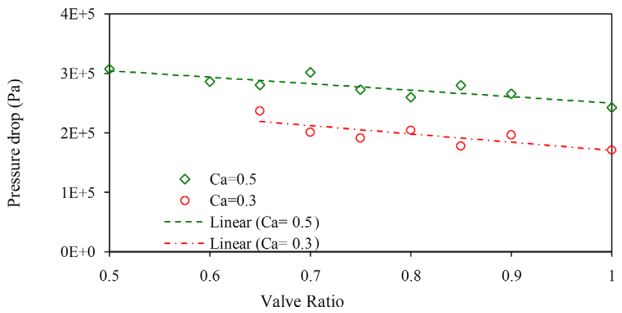

Fig. 18 Pressure drop as a function of valve ratio for the nanoscale case. In the diagram the pressure drop is calculated at the breakup moment.

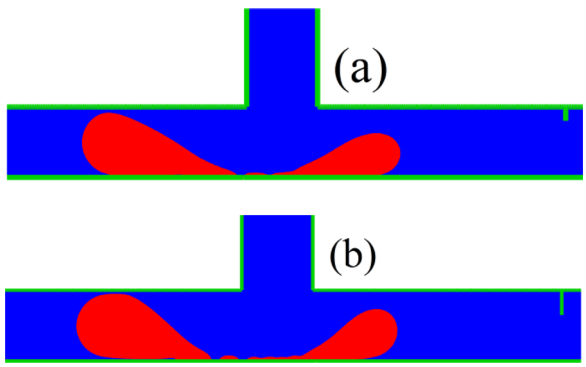

Fig. 19 Droplet breakup for the nanoscale case. (*a*) Ca = 0.3 and valve ratio = 0.8. (*b*) Ca = 0.5 and the valve ratio = 0.65. As can be seen in both the cases, the tunnel does not form. Therefore, by the increase of the valve ratio, the pressure drop reduces linearly.

for reducing the pressure drop, the capillary number should be decreased and the valve ratio should be increased.

Conclusion

A T-junction with a valve for producing unequal-sized droplets was studied. The main advantage of this method is that, after manufacturing of the system, one can simply control the size of generated droplets by tuning the valve. A VOF numerical algorithm was used to inspect the system. The results of the T-junction with valve for systems at the microscales and nanoscales were presented. The influence of the valve ratio and the capillary number on the volume ratio of the generated droplets was presented, and it was observed that at both the microscales and nanoscales in a specific valve ratio, with reduction of the capillary number, a smaller droplet is generated in the branch with valve. Two parameters, namely, breakup time (for increasing the droplet generation rate) and breakup length (for reducing the system cost) were introduced and influence of the capillary number and the valve ratio on them was investigated. The results revealed that at both the microscales and nanoscales, the breakup time is independent of the valve ratio and for reducing it the capillary number should be increased. Also, it was found that the breakup length of the droplets at both the micro- and nanoscale is independent of the valve ratio, but at the microscale case reduces by decreasing the capillary number and at the nanoscale case it is independent of the capillary number. The influence of the valve ratio and the capillary number on the pressure drop of the system was studied and it was shown that at the microscales and nanoscales, in the breakup moment if the tunnel is formed, the pressure drop is independent of the valve ratio. Otherwise, the pressure drop reduces linearly by increasing the valve ratio. Our results indicated that 2D and 3D numerical results are very close for all the cases considered (the difference is less than 10%). Therefore, since 3D cases are computationally demanding, 2D calculations can be reasonably used for this purpose.

References

[1] Christopher, G. F., Noharuddin, N. N., Taylor, J. A., and Anna, S. L., 2008, "Experimental Observations of the Squeezing-to Dripping Transition in T-Shaped Microfluidic Junctions," Phys. Rev. E., **78**, p. 036317.

[2] Tice, J., Song, H., Lyon, A., and Ismagilov, R., 2003, "Formation of Droplets and Mixing in Multiphase Microfluidics at Low Values of the Reynolds and the Capillary Numbers," Langmuir, **19**(22), pp. 9127–9133.

[3] Dupin, M. M., Halliday, I., and Care, C. M., 2006, "Simulation of a Microfluidic Flow-Focusing Device," Phys. Rev. E., **73**, p. 055701.

[4] Liu, H., and Zhang, Y., 2011, "Droplet Formation in Microfluidic Cross-Junctions," Phys. Fluids, **23**, p. 082101.

[5] Liu, H., and Zhang, Y., 2011, "Lattice Boltzmann Simulation of Droplet Generation in a Microfluidic Cross-Junction," Commun. Comput. Phys., **9**(5). pp. 1235–1256.

[6] Wu, L., Tsutahara, M., Kim, L. S., and Ha, M. Y., 2008, "Three-Dimensional Lattice Boltzmann Simulations of Droplet Formation in a Cross-Junction Microchannel," Int. J. Multiphase Flow, **34**(9), pp. 852–864.

[7] Wang, P., Gao, W., Cao, Z., Liechti, K. M., and Huang, R., 2013, "Numerical Analysis of Circular Graphene Bubbles," ASME J. Appl. Mech., **80**(4), p. 040905.

[8] Leshansky, A. M., and Pismen, L. M., 2009, "Breakup of Drops in a Microfluidic T-junction," Phys. Fluids, **21**, p. 023303.

[9] Deremble, L. M., and Tabeling, P., 2006, "Droplet Breakup in Microfluidic Junctions of Arbitrary Angles," Phys. Rev. E, **74**, p. 035303.

[10] Link, D. R., Anna, S. L., Weitz, D. A., and Stone, H. A., 2004, "Geometrically Mediated Breakup of Drops in Microfluidic Devices," Phys. Rev. Lett., **92**, p. 054503.

[11] Nguyen, H., Wang, S., Mohan, R. S., Shoham, O., and Kouba, G., 2014, "Experimental Investigations of Droplet Deposition and Coalescence in Curved Pipes," ASME J. Energy Resour. Technol., **136**(2), p. 022902.

[12] Muradoglu, M., and Gokaltun, S., 2004, "Implicit Multigrid Computations of Buoyant Drops Through Sinusoidal Constrictions," ASME J. Appl. Mech., **71**(6), pp. 857–865.
[13] Carroll, B., and Hidrovo, C., 2013, "Droplet Detachment Mechanism in a High-Speed Gaseous Microflow," ASME J. Fluids Eng., **135**(7), p. 071206.
[14] Li, S., Li, H. Z., Ma, Y., Jiang, S., Fu, T., and Zhu, C., 2012, "The Drag Coefficient and the Shape for a Single Bubble Rising in Non-Newtonian Fluids," ASME J. Fluids Eng., **134**(8), p. 084501.
[15] Ramdin, M., and Henkes, R., 2012, "Computational Fluid Dynamics Modeling of Benjamin and Taylor Bubbles in Two-Phase Flow in Pipes," ASME J. Fluids Eng., **134**(4), p. 041303.
[16] Jayaprakash, A., Hsiao, C. T., and Chahine, G., 2012, "Numerical and Experimental Study of the Interaction of a Spark-Generated Bubble and a Vertical Wall," ASME J. Fluids Eng., **134**(3), p. 031301.
[17] Das, A. K., Thome, J. R., and Das, P. K., 2009, "Transition of Bubbly Flow in Vertical Tubes: Effect of Bubble Size and Tube Diameter," ASME J. Fluids Eng., **131**(9), p. 091304.
[18] Bedram, A., and Moosavi, A., 2013, "Breakup of Droplets in Micro and Nanofluidic T-Junctions," J. Appl. Fluid Mech., **6**, pp. 81–86.
[19] Sehgal, B. R., Nourgaliev, R. R., and Dinh, T. N., 1999, "Numerical Simulation of Droplet Deformation and Break-up by Lattice Boltzmann Method," Prog. Nucl. Energy, **34**(4), pp. 471–488.
[20] Choi, J. H., Lee, S. K., Lim, J. M., Yang, S. M., and Yi, G. R., 2010, "Designed Pneumatic Valve Actuators for Controlled Droplet Breakup and Generation," Lab Chip, **10**(4), pp. 456–461.
[21] Ting, T. H., Yap, Y. F., Nguyen, N. T., Wong, T. N., Chai, J. C. K., and Yobas, L., 2006, "Thermally Mediated Breakup of Drops in Microchannels," Appl. Phys. Lett., **89**(23), p. 234101.
[22] Bedram, A., and Moosavi, A., 2011, "Droplet Breakup in an Asymmetric Microfluidic T-Junction," Eur. Phys. J. E., **34**(8), pp. 1–8.
[23] Nie, J., and Kennedy, R. T., 2010, "Sampling From Nanoliter Plugs Via Asymmetrical Splitting of Segmented Flow," Anal. Chem., **82**(18), pp. 7852–7856.
[24] Zhu, H.-W., Zhang, N.-G., He, R.-X., Li, S.-Z., Guo, S.-S., Liu, W., and Zhao, X.-Z., 2011, "Controllable Fission of Droplets and Bubbles by Pneumatic Valve," Microfluidics Nanofluidics, **10**(6), pp. 1343–1349.
[25] Lafaurie, B., Nardone, C., Scardovelli, R., Zaleski, S., and Zanetti, G., 1994, "Modeling Merging and Fragmentation in Multiphase Flows With SURFER," J. Comput. Phys., **113**(1), pp. 134–147.
[26] Bretherton, F. P., 1961, "The Motion of Long Bubbles in Tubes," J. Fluid Mech., **10**(2), pp. 166–188.
[27] Jensen, M. J., 2002, "Bubbles in Microchannels," M.S. thesis, Technical University of Denmark, Lyngby, Denmark.
[28] Navier, C. L. M. H., 1823, "M'emoire sur les lois du Mouvement des Fluides," Mém. Acad. R. Sci. Inst. Fr., **6**, pp. 389–440.